Interaction of point defects with twin boundaries in Au: A molecular dynamics study

Fayyaz Hussain[a)], Sardar Sikandar Hayat[a)b)], Zulfiqar Ali Shah[b)†], Najmul Hassan[b)], and Shaikh Aftab Ahmad[a)]

[a)] *Department of Physics, The Islamia University of Bahawalpur, Bahawalpur* 63120, *Pakistan*
[b)] *Department of Physics, Hazara University, Mansehra* 21300, *Pakistan*

(Received 5 October 2012; revised manuscript received 2 April 2013)

The molecular dynamics simulation technique with many-body and semi-empirical potentials (based on the embedded atom method potentials) has been used to calculate the interactions of point defects with (1 1 1), (1 1 3), and (1 2 0) twin boundaries in Au at different temperatures. The interactions of single-, di-, and tri-vacancies (at on- and off-mirror sites) with the twin interfaces at 300 K are calculated. All vacancy clusters are favorable at the on-mirror arrangement near the (1 1 3) twin boundary. Single- and di-vacancies are more favorable at the on-mirror sites near the (1 1 1) twin boundary, while they are favorable at the off-mirror sites near the (1 2 0) twin boundary. Almost all vacancy clusters energetically prefer to lie in planes closest to the interface rather than away from it, except for tri-vacancies near the (1 2 0) interface at the off-mirror site and for 3.3 and 3.4 vacancy clusters at both sites near the (1 1 1) interface, which are favorable away from the interface. The interaction energy is high at high temperatures.

Keywords: molecular dynamics, twin boundaries, vacancy clusters, gold

PACS: 61.72.Bb, 61.72.Mm, 61.43.Bn, 61.72.Ji **DOI:** 10.1088/1674-1056/22/9/096102

1. Introduction

Gold (Au) is now being used in electronics,[1] industrial sectors, nanotechnology, and particularly nanophotonics.[1] Gold and gold alloys have also been used as catalysts.[2–4] A gold-coated bipolar plate provides an effective way of producing electrical conductivity and corrosion results. Gold is being used to increase the data storage capacity of devices which use memory disks and flash drives.[5] Metallic bipolar plate technology with thin gold-coated stainless steel has also been developed.[6,7] Other examples include gold nanodots and gold nanorods.[8]

The interaction between crystal defects plays a very crucial role in many theories of the strength of materials. The formation of cavities, denuded zones, and grain-boundary precipitates express these effects in a striking manner. As for the mechanism of atom transport in an age hardening alloy, it is observed that the interaction plays a very significant role. The interaction between solute atoms and vacancies in metal has been the subject of study in recent years. The energies and structures of close packed vacancy clusters have been discussed in many early studies.[9–11] Unfortunately, the elasticity theory cannot be used to investigate the interaction energy. Therefore, clearly relativistic results of interaction between different defects can be obtained using simulation tools.

The grain-boundary shuffling mechanism in nano-crystalline fcc metals using the molecular dynamics (MD) method has been studied by Swygenhoven and Derlet.[12] Daw and Baskes[13] have developed the embedded-atom method (EAM) potentials. The EAM method potentials have been used for the study of grain boundaries in bcc and fcc metals and in other applications such as deformation of fcc nanowires by twining and slip.[14,15] Based on these potentials and the MD (which is used in this project), different studies have been presented for metals.[16–19]

Point defects have a significant role in controlling characteristics such as plasticity, strength, and electrical and thermal conductivities.[20] Point defects provide the fast grain-boundary diffusion in grain boundaries. Studies of grain boundaries show structural effects associated with point defects, like the delocalization of vacancies as well as the vacancy instability at certain grain-boundary sites and interstitial in grain-boundary core.[21] The interaction of point defects with twin boundaries may contribute to the change in mechanical property. Bacon and Osetsky[22] have studied the atomic-scale processes involved in dislocation–defect interactions extensively. The strength and rupture properties of materials can be manipulated strongly by the isolation of impurity atoms from grain-boundaries or other interfaces. Restrictions on twin-boundary motion and intensification by pinning twinning dislocations may be caused by the result of point-defect clusters. Serra and Bacon[23] have shown that the moving boundaries can act as recombination centers or sinks for defects and can provide resources to remove defects from regions of radiation damage.

For nano-crystalline materials, the most fundamental deformation mode is grain-boundary sliding at room

†Corresponding author. E-mail: sikandariub@yahoo.com

temperature.[24,25] Twining is a common sort of planar defect which has been frequently observed in fcc metals.[26–28] There are four possible distinct tri-vacancies and a single di-vacancy cluster configuration in the (1 1 1) plane of an fcc crystal.[29] The interactions existing between low index twins and vacancies are attractive in fcc metal.[30–32] The temperature dependence of the (1 1 1) twin boundary energy was reported in a very early work.[33] The static calculations for interaction energies with low-index twin-boundaries are available,[32] but the field still requires an explanation of the interactions of point defects with twin boundaries at high temperatures, then things can be more reliable (approaching reality) when the atomic dynamics is involved. Attention is focused on the interaction of small vacancy clusters with (1 1 1), (1 1 3), and (1 2 0) twin boundaries, which are well known and have been discussed in different studies.[12,13,26–28,32] The interplanar spacings of (1 1 1), (1 1 3), and (1 2 0) planes are 0.5773α, 0.3015α, and 0.2236α, respectively. The above said importance of interactions of defects and the use of Au in the industrial sector motivate us to calculate these interactions. Low index twin boundaries such as (1 1 1), (1 1 3), and (1 2 0) are selected in this study because they are of scientific importance,[18,19,29–33] easy to develop conventional geometric structures, and they also behave as stable models in simulation.

The rest of the present paper is arranged as follows. Section 2 carries the salient features of the technique. Steps of the procedure involved in the simulation work are explained. In Section 3, the results of MD simulation are discussed for interaction energies at 300 K along with details of twins. A graphical presentation of calculations is also made. Finally, the conclusions of this work are presented in Section 4.

2. Details of calculation

The routines for generating the lattice and twin boundaries are introduced in the dyn86 molecular dynamics simulation code. The details of the MD technique can be found in many books and articles.[13,16–19] The salient features of the technique are as follows. In this code, the Nordsiesk algorithm[34] is used with a time step of 10^{-15} s. To generate the crystal lattice at any desired temperature, the temperature is increased using the condition of a constant number of atoms, pressure, and temperature (*NPT* ensemble). The computational cell used consists of 256 atoms arranged in an fcc lattice with lattice parameter 4.08 Å at 0 K. The EAM potentials developed by Daw and Baskes[13] have cut-off radius $R_c \approx 5.55$ Å. To attain the lattice parameter at desired temperatures, we use[17]

$$a = (4\Omega)^{1/3},$$

where Ω is the calculated average atomic volume at each temperature. The computational cell is generated at a specific temperature while keeping the pressure constant. The system is allowed to evolve till the cell edges and volume become constant. The convergences of lattice parameter and energy per atom with respect to the system size are checked. The use of periodic boundary conditions in all directions diminishes the effect of the size of the crystal on the calculation of the lattice parameter.

For the desired direction in which the twin boundary is generated, the fixed boundary condition is applied. Fixed boundaries produce surfaces in these directions at the boundary of crystal, otherwise the defect (twin boundary) will be repeated infinitely with the use of periodic boundary conditions. To minimize the effect of the fixed boundaries on the twin formation energy, enough planes must be taken along these directions. The energy and atomic structure of the model are monitored. To study the twin boundaries, a three-dimensional model of crystallite is generated in the form of a rectangular block of atoms, like a slab with suitable mutually perpendicular axes. The energy of a perfect crystal (E_P) is calculated in the first step, then a twin interface is introduced in a desired plane of the computational cell. The energy of a crystal with twin-boundary (E_{P+T}) is calculated again using the condition of a constant number of atoms, volume, and energy (*NVE* ensemble). In the first step, the crystal is allowed to relax to minimize its energy using the conjugate gradient method,[35] and then the relax energy of twin (E_T) is calculated using the following relation:[19]

$$E_T = E_{P+T} - E_P.$$

To create a single-vacancy cluster, an atom is replaced by a vacancy. Similarly, to create a di-vacancy, two atoms (nearest neighbor atoms in the (1 1 1) plane) are replaced by two vacancies. The procedure to create a tri-vacancy (3.1, 3.2, 3.3, and 3.4 vacancy clusters in the (1 1 1) plane) has been explained[29] and graphically represented by Ahmad and Ramzan.[32] Firstly, a vacancy cluster is introduced in the nearest plane to the twin boundary to study the interaction of vacancy clusters with twin boundaries and then in the next planes away from it. For those vacancy clusters which do not exist in a single plane, at least one vacancy of those clusters has to be taken into consideration of vicinity plane from twin. For each case, the twin–vacancy interaction energy is calculated. The energy E_V associated with a single-vacancy is given by[32]

$$E_V = E_{P+V} - E_P,$$

where E_{P+V} gives the energy of the crystal containing a single vacancy. If N represents the number of atoms in a vacancy cluster, then the energy E_{NV} associated with N vacancies (di- or tri-vacancy) is calculated using the relation[36]

$$E_{NV} = E_{P+NV} - NE_V - E_P,$$

where E_{P+NV} gives the energy of the crystal containing N vacancies. In the case of two or more vacancies, the interaction of vacancies is added.[36] We have to find the energies of both twin boundary and vacancy. The interaction energy between the twin boundary and N vacancies is calculated using the following relation:[36]

$$E_C^N = E_{P+T+NV} - E_{P+T} - E_{NV},$$

where E_{P+T+NV} is the energy of the crystal in the presence of N vacancies and a twin boundary. The value of N may be taken to be 1, 2, or 3 according to the size of the vacancy cluster.

The interlayer spacing along the three directions of the lattice is taken into account. The original positions of the atomic planes have to be shuffled to generate the twin boundary in the crystal. This generates a disturbance of atomic distances near the twin boundaries of the crystal. After generating the defect, the computational cell is allowed to relax (i.e., it tends to be decoupled with the interaction energy). Atoms tend to be rearranged to nullify the high energy of the grain boundary. During relaxation, the atoms near the twin boundaries move in order of nanometer and gain minimum energy. After the relaxation of atoms, the interplanar spacing is again calculated. The change in interplanar separation is determined. To calculate the percentage of interlayer relaxation $(d_{i,i+1})$ near the twin boundary, we use[18]

$$d_{i,i+1} = \frac{[(Y_{i+1} - Y_i) - d_b]}{d_b} \times 100\%,$$

where Y is the direction perpendicular to the twin boundary, and the bulk interplanar spacing is d_b. The percentage of plane registry relaxation (r_i) of i-th plane near the twin boundary can be calculated as[18]

$$r_i = \frac{(X_{final} - X_{initial})}{r_b} \times 100\%,$$

where X is the direction in which the whole plane is moved, and r_b is the bulk interlayer spacing.

3. Results and discussion

An experimental lattice parameter of 4.08 Å is used to generate a Au fcc crystal at 0 K with 256 atoms. Using the preliminary NPT simulation, the crystals are generated at different temperatures. This provides the lattice parameter α at different temperatures, which is used to develop a slab like structure with the required geometry of planes for the twin boundaries. The lattice parameter for Au at different temperatures is calculated using these potentials.[37] The calculated lattice parameters agree well with the experimental values (see Ref. [37] for graphical representation).

3.1. Plane (1 1 1) twin boundary

The crystallite with 1080 atoms is developed for the (1 1 1) twin boundary. This is a rectangular block of atoms with faces (1 1 $\bar{2}$), (1 1 1), and (1 $\bar{1}$ 0). The computational cell has 18 (1 1 $\bar{2}$), 90 (1 1 1), and 4 (1 $\bar{1}$ 0) planes. The interplanar spacings are 0.833 Å, 2.36 Å, and 1.44 Å along [1 1 $\bar{2}$], [1 1 1], and [1 $\bar{1}$ 0] directions, respectively. The (1 1 1) twin formation energy is 4.07 mJ/m^2 at 0 K. The twin formation energies at different temperatures up to 1200 K, in steps of 100 K, are given in Fig. 1. For the (1 1 1) twin interface, the upper half of the crystal is shuffled in the following way: taking into account the [1 1 1] direction from the middle of the crystal, the first plane is moved positive and the second is moved negative one interplanar spacing (0.833 Å) along the [1 1 $\bar{2}$] direction, while the third plane remains unchanged. For the next 3 planes (4, 5, and 6), the same pattern is repeated with keeping the [1 1 1] directions under rigid boundary condition, while others under periodic boundary conditions. The relaxed structure of the (1 1 1) twin boundary projected on the (1 $\bar{1}$ 0) plane has been presented in the previous work.[18] Interlayer and registry relaxations are not found around the (1 1 1) twin boundary due to the high atomic density and larger interplanar spacing of the (1 1 1) plane, and very small shuffling required to create the (1 1 1) twin-boundary, which has already been suggested for Pd, Pt, and Al.[18,19]

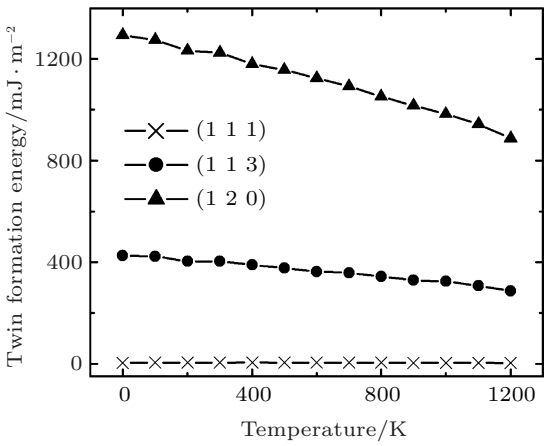

Fig. 1. Twin formation energies for the (1 1 1), (1 1 3), and (1 2 0) twin boundaries at different temperatures. Plot lines for (1 1 3) and (1 2 0) interfaces show that with the increase in temperature the twin formation energy decreases.

To determine the interaction energy for cluster 1.1, a single vacancy is introduced near the (1 1 1) twin boundary on either side in the first plane at 300 K, then the interaction energy is calculated. The interaction energy for cluster 1.1 in the first plane near the (1 1 1) twin boundary is 0.0084 eV. This process is repeated for the next 2–8 planes. It is observed that the values of interaction energy are positive in all planes. This shows the repulsive behavior for the single vacancy. The single vacancy is more repulsive in the first plane but less repulsive

in the second one (with an interaction energy of 0.00743 eV) than that in all other planes. Similarly, cluster 2.1 is generated near the (1 1 1) twin boundary by introducing two vacancies. The second vacancy is generated at distance 0.835 Å (one interplanar spacing on the (1 1 1) plane) with the first vacancy along the [1 1 $\bar{2}$] direction. The interaction energy for cluster 2.1 in the first plane near the (1 1 1) twin boundary is 0.01346 eV. The di-vacancy is repulsive almost in all 1–8 planes and less repulsive in the fourth plane (with an interaction energy of 0.00949 eV) than that in all other planes. The tri-vacancy is generated with different geometries, which are 3.1, 3.2, 3.3, and 3.4 at 300 K (see Ref. [32]). The interaction energies of clusters 3.1, 3.2, 3.3, and 3.4 with the (1 1 1) twin boundary in the first plane are 3.44741 eV, 3.11035 eV, 3.34667 eV, and 1.02761 eV, respectively. Clusters 3.1, 3.2, and 3.3 are repulsive in all planes. This repulsion is high in the first plane. Cluster 3.4 is subjected to a small repulsion in the closest plane but attraction in 2–8 planes.

Two single- and di-vacancies are generated on both sides of the twin interface at on- and off-mirror positions. To obtain the off-mirror position, single- and di-vacancies are shifted by one interplanar spacing ($T_x = 0.833$ Å) along [1 1 $\bar{2}$]. On- and off-mirror positions are repulsive for both single- and di-vacancies but less repulsive in the first plane than that in all other planes. The single vacancy behaves the same at on- and off-mirror sites for 2–8 planes. The di-vacancy shows less repulsion in the second plane and more repulsion in the third, fourth, and fifth plane at the off-mirror position than that at the on-mirror position, and the same behavior is found in the sixth, seventh, and eighth plane. The tri-vacancies are also calculated in the pair form at on- and off-mirror positions. The tri-vacancy clusters are repulsive in the first plane at both on- and off-mirror sites. This repulsion is increased for clusters 3.1 and 3.2 and decreased for clusters 3.3 and 3.4 at the second plane, and then the interaction almost remains the same in 2–8 planes. The values of interaction energy near the (1 1 1) twin boundary at 0 K are comparable with the results given by Ahmad and Ramzan.[32] The plots in Ref. [32] have the same trend as the interaction energy calculated, but small differences in magnitude are found due to different metals and temperatures for the calculations (see Ref. [32] for graphical representation).

The effects of temperature on the interaction energy for clusters 1.1, 2.1, and 3.1 are calculated near the (1 1 1) twin boundary in the first pane and illustrated in the temperature range of 0–1000 K, in steps of 100 K, in Figs. 2–4, respectively. With the increase in temperature, there are no considerable effects on the interaction energy for clusters 2.1 and 3.1. While for cluster 1.1, the repulsion with the (1 1 1) twin boundary decreases with the increase in temperature (by an average value of −0.00085 eV for 100 K), and it shows an

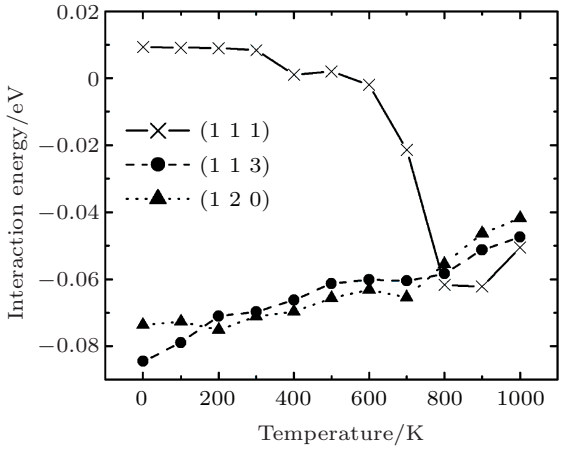

Fig. 2. Interaction energies of a single-vacancy cluster in the first plane near the (1 1 1), (1 1 3), and (1 2 0) twin boundaries in the temperature range of 0–1000 K.

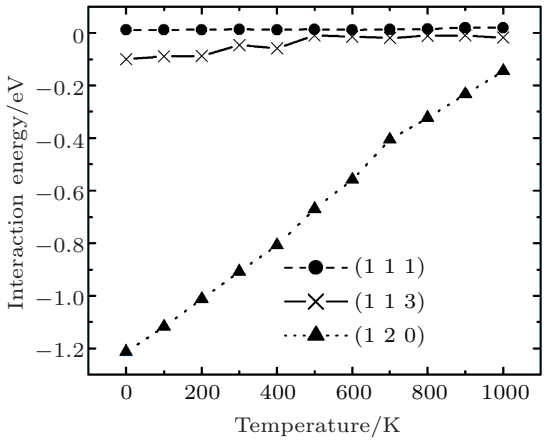

Fig. 3. Interaction energies of di-vacancy cluster at the first plane near the (1 1 1), (1 1 3), and (1 2 0) twin boundaries in the temperature range of 0–1000 K.

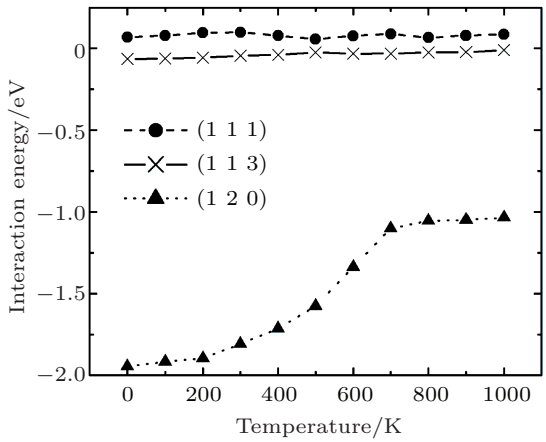

Fig. 4. Interaction energies of tri-vacancy cluster in the first plane near the (1 1 1), (1 1 3), and (1 2 0) twin boundaries in the temperature range of 0–1000 K.

attractive behavior at 600 K. At low temperature, due to the high atomic density of the (1 1 1) plane, the relaxation of atoms is difficult and the single vacancy faces repulsion. With the increase in temperature, the interlayer separation and distances between the atoms increase, and the relaxation takes

place easily. Further increase in temperature induces more attraction for the 1.1 vacancy cluster with interface and shows (maximum attraction) interaction energy −0.062 eV at 900 K. At 1000 K, a small decrease in attraction is observed.

3.2. Plane (1 1 3) twin boundary

The computational cell with 880 atoms for the (1 1 3) twin boundary consists of (3 3 $\bar{2}$), (1 1 3), and (1 $\bar{1}$ 0) planes. The simulation cell at 0 K has 44 (3 3 $\bar{2}$) planes with interplanar spacing of 0.87 Å, 110 (1 1 3) planes with interplanar spacing of 1.23 Å, and 4 (1 $\bar{1}$ 0) planes with interplanar spacing of 1.44 Å.

To generate the twin boundary in the middle of the computational cell, the upper half of the crystal is shuffled in the following manner: taking into account the [1 1 3] direction from the middle of the crystal, the first plane is moved positive, while the tenth plane is moved negative ten interplanar spacings of the [3 3 $\bar{2}$] direction (8.72 Å); the second plane is moved negative, while the ninth plane is moved positive two interplanar spacings of the [3 3 $\bar{2}$] direction (1.64 Å); the third plane is moved positive, while the eighth plane is moved negative eight interplanar spacings of the [3 3 $\bar{2}$] direction (6.96 Å); the fourth plane is moved negative, while the seventh plane is moved positive four interplanar spacings of the [3 3 $\bar{2}$] direction (3.49 Å); the fifth plane is moved positive, while the sixth plane is moved negative six interplanar spacings of the [3 3 $\bar{2}$] direction (5.19 Å). The same sequence is repeated in the next ten (11–20) planes along the [1 1 3] direction in the same way.

Fixed boundaries are applied along the [1 1 3] direction, while the other directions have periodic boundaries. The twin formation energy for the (1 1 3) twin is 450.97 mJ/m^2 at 0 K. The twin formation energy for the (1 1 3) interface at different temperatures (0–1200 K) is given in Fig. 1. The twin formation energy of the (1 1 3) twin boundary decreases by an average of 11.71 mJ/m^2 with an increase of 100 K. The relaxed (1 1 3) twin-interface structure projected on the (1 $\bar{1}$ 0) plane has been presented in Refs. [18] and [19].

The maximum relaxation of interlayer separation is of d_{01} spacing (between interface and first plane), which is about 8% expansion. Similarly, the maximum contraction is about 6% of d_{12} spacing (between the first and the second planes). The maximum percentage of registry relaxation in r_2 (second plane from the interface) is about 4% along the [3 3 $\bar{2}$] direction. The multilayer relaxation behavior near the (1 1 3) twin boundary oscillatorily extends through the layers (+,-,+, ...); while the plane registry relaxation has no regular order. These results of relaxation are comparable to the early finding.[18]

To calculate the interaction energy at 300 K for cluster 1.1, a single vacancy is introduced in the closest (first) plane on either side of the (1 1 3) twin boundary. The interaction energy for cluster 1.1 in the first plane near the (1 1 3) twin boundary is −0.0697 eV (attractive). This process is repeated for the next 2–8 planes. The interaction energy is less than zero in all planes. This shows an attractive behavior for a single vacancy in all planes. The single vacancy is more attractive in the second plane with an interaction energy of −0.08442 eV and less attractive with an interaction energy of −0.06782 eV in the fifth plane than in all other planes (see Fig. 5(a)). The average variation in the interaction energy of the single vacancy is ±0.008721 eV. Similarly, cluster 2.1 is generated near the (1 1 3) twin boundary by introducing two vacancies. The interaction energy for cluster 2.1 in the first plane near the (1 1 3) twin boundary is −0.0458 eV at 300 K, which is more attractive than that in all other planes. The di-vacancy is attractive in all 1–8 planes and less attractive in the third plane (with an interaction energy of -0.03896 eV) than that in all other planes (see Fig. 5(a)). The average variation in the interaction energy of the di-vacancy is ± 0.023371 eV. Figure 5(b) presents the results of interaction energy at 300 K for the tri-vacancy with different geometries 3.1, 3.2, 3.3, and 3.4. The interaction energies of clusters 3.1, 3.2, 3.3, and 3.4 with the (1 1 3) twin boundary are −0.04524 eV, 0.00162 eV, −0.17415 eV, and −0.17123 eV, respectively, in the first plane. Cluster 3.2 is repulsive almost

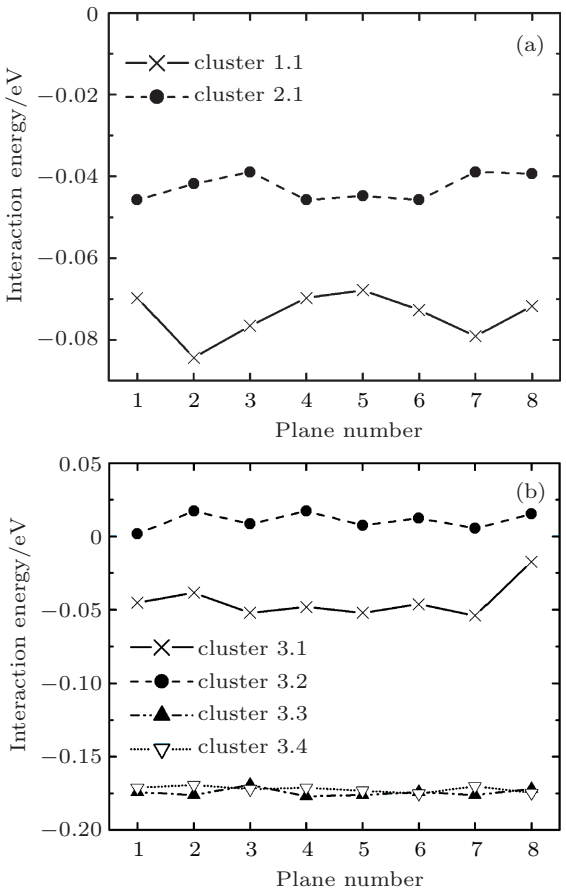

Fig. 5. Interaction energies of (a) single and di-vacancies and (b) four tri-vacancy clusters against the plane number near the (1 1 3) twin boundary at 300 K.

in all planes with a small variation in magnitude. Clusters 3.1, 3.3, and 3.4 are attractive in all planes with a small variation in interaction energy. Cluster 3.1 is less attractive in all planes than clusters 3.3 and 3.4.

Single- and di-vacancies are also generated on both sides of the twin interface at on- and off-mirror positions. To obtain the off-mirror position, single- and di-vacancies are shifted by $T_x = 0.87$ Å (one interplanar spacing) along [3 3 $\bar{2}$]. Clusters 1.1 and 2.1 present (throughout) an attractive behavior at off-mirror positions and a repulsive behavior at on-mirror positions, as given in Figs. 6(a) and 6(b). Single- and di-vacancies are less repulsive at on-mirror position and more attractive at off-mirror position at plane numbered as 1, and for beyond planes, this repulsion slightly increases (attraction slightly decreases with small fluctuations). Similarly, tri-vacancies are also calculated in the pair form at on- and off-mirror positions. The interaction energies of tri-vacancy at 300 K on either side of the (1 1 3) twin boundary at on- and off-mirror sites are plotted in Figs. 7(a) and 7(b). At on-mirror sites, the tri-vacancy clusters are attractive in the first plane, and this attraction reduces in the second plane and almost the same with small variations up to the eighth plane (see Fig. 7(a)). At off-mirror sites, all tri-vacancy clusters are repulsive (see Fig. 7(b)). This repulsion increases in the second plane up to the eighth plane for all tri-vacancy clusters. Clusters 3.1 and 3.4 are more repulsive than clusters 3.2 and 3.3.

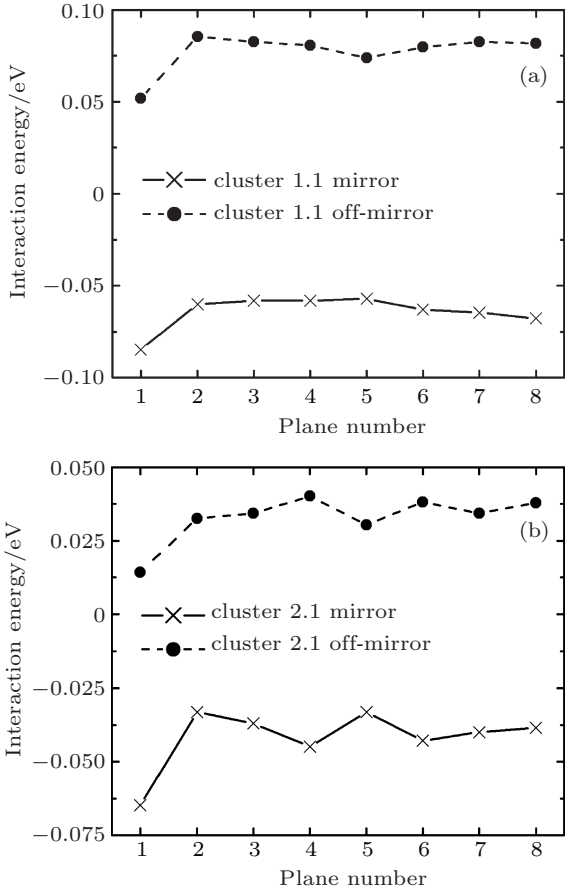

Fig. 6. Interaction energies of (a) single-vacancy and (b) di-vacancy clusters on either side of the (1 1 3) twin boundary at 300 K.

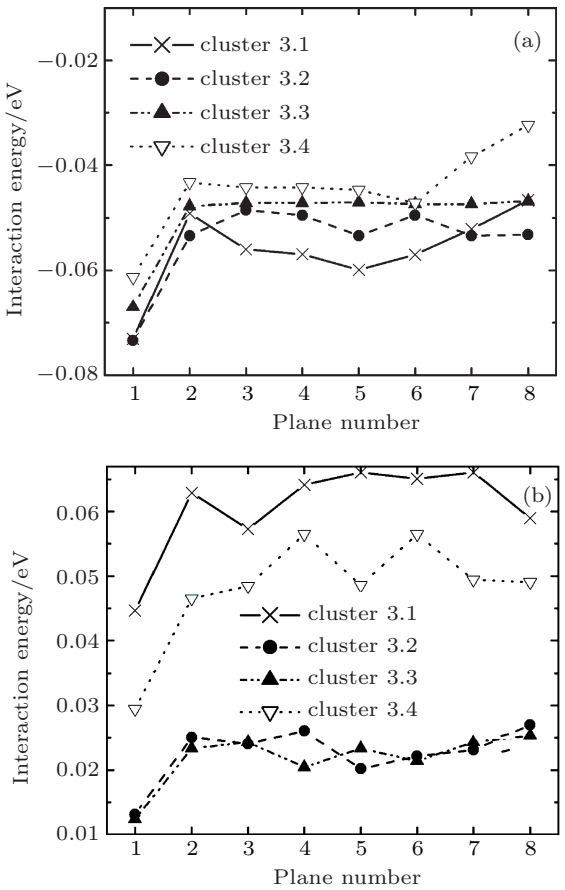

Fig. 7. Interaction energies of tri-vacancy clusters at 300 K on either side of (1 1 3) twin boundary at (a) on- and (b) off-mirror sites.

The interaction energies for clusters 1.1, 2.1, and 3.1 near the (1 1 3) twin boundary in the first pane in the temperature range of 0–1000 K, in steps of 100 K, are plotted in Figs. 2–4, respectively. Clusters 1.1, 2.1, and 3.1 have the interaction energies of −0.08455 eV, −0.09987 eV, and −0.06432 eV, respectively, at 0 K. The increase in temperature has considerable effects on the interaction energy for all vacancy clusters. The interaction energy averagely increases by 0.007686 eV, 0.009079 eV, and 0.005847 eV (for 100 K increase in temperature) for clusters 1.1, 2.1, and 3.1, respectively. This increasing trend is more prominent for di-vacancy near the (1 1 3) twin boundary. At 1000 K, the interaction energies become −0.04743 eV, -0.01812 eV, and −0.01104 eV for clusters 1.1, 2.1, and 3.1, respectively. It means that at 0 K all the vacancy clusters are attractive, while with the increase in temperature this attraction decreases.

3.3. Plane (1 2 0) twin boundary

A rectangular block of 960 atoms is used for the (1 2 0) twin boundary with mutually perpendicular 30 (2 $\bar{1}$ 0), 160 (1 2 0), and 2 (0 0 1) planes at 0 K. The 9.12 Å is the interplanar spacing along [2 $\bar{1}$ 0] and [1 2 0] directions, while 2.04 Å is the spacing along the [0 0 1] direction. The relaxed (1 2 0) twin

structure projected on the (0 0 1) plane can be seen in Ref. [18]. The relaxed twin formation energy at 0 K is 1293.52 mJ/m^2. Averagely 33.86 mJ/m^2 twin formation energy decreases with 100 K increase in temperature. The twin formation energy for the (1 2 0) twin interface in the temperature range of 0–1200 K, in steps of 100 K, is given in Fig. 1.

To generate the (1 2 0) twin interface, the upper half of the crystal is shuffled along the [1 2 0] direction in the following manner: considering from the middle of the crystal, the first plane is moved four inter planar spacings (3.67 Å) along negative, the second plane is moved two interplanar spacings (1.82 Å) along positive, the third plane is moved two interplanar spacings along negative, the fourth plane is moved four inter planar spacings along positive [2 $\bar{1}$ 0] direction, and the fifth plane remains unchanged. The same sequence is repeated in the next five 6–10 planes along the [1 2 0] direction.

A single vacancy is created (firstly) in plane 1 (closest plane) near the (1 2 0) twin boundary on either side at 300 K and then it is generated in turn in the next planes (2, 3, ..., 8) away from the twin interface. The interaction energy with twin is calculated for each case. The single vacancy has an interaction energy of −0.11146 eV in the first plane at 300 K. Figure 8(a) shows that cluster 1.1 presents an attractive behavior in the first, second, and seventh planes, while in all other planes its behavior is repulsive with more repulsion in the fourth pale (with an interaction energy value of 0.05993 eV). Similarly, the di-vacancy is generated near the (1 2 0) twin boundary by generating two vacancies. The interaction energy for cluster 2.1 in the first plane at 300 K is −1.08788 eV. The di-vacancy is repulsive beyond the third plane up to the eighth plane and more repulsive in the fourth plane (with an interaction energy value of 0.09789 eV) than that in all other planes (see Fig. 8(a)). The interaction energy of four tri-vacancy clusters against the plane number near the (120) twin boundary at 300 K is given in Fig. 8(b). The interaction energies of clusters 3.1, 3.2, 3.3, and 3.4 are −1.80849 eV, −2.09657 eV, −0.55262 eV, and −1.73817 eV, respectively, in the first plane. All four tri-vacancies are subjected to attraction in planes 1 and 2. This attraction is low for cluster 3.3 and high for cluster 3.2.

A pair of single- and di-vacancies is generated on both sides of the twin interface at on- and off-mirror positions. To obtain the off-mirror position, single- and di-vacancies are shifted by $T_x = 9.12$ Å (one interplanar spacing) along [2 $\bar{1}$ 0]. Figures 9(a) and 9(b) show that at off-mirror positions, clusters 1.1 and 2.1 are attractive in the first and the sixth planes and cluster 1.1 also has small attractions in the seventh and the eighth planes, while they are repulsive in all other planes. In the case of on-mirror positions, these clusters present repulsive behaviors in all planes. However, the di-vacancy is more repulsive than the single vacancy in all planes at the on-mirror positions. The on-mirror position is less repulsive in the second plane for di-vacancy and in the fourth and the fifth planes for single vacancy than the off-mirror position. Similarly, tri-vacancies are also calculated in the pair form at on- and off-mirror positions. The interaction energies of tri-vacancy cluster on either side of the (1 2 0) twin boundary at on- and off-mirror sites are represented in Figs. 10(a) and 10(b). At on- and off-mirror sites, the tri-vacancy clusters are repulsive in the first plane. This repulsion increases for the on-mirror sites in the second plane for all tri-vacancy clusters and decreases in the case of the off-mirror sites for all tri-vacancy clusters in the third plane. The interaction energies at the on-mirror positions for clusters 3.1 and 3.4 in the third and the fourth planes are high and then gradually decrease with small variations for clusters 3.1, 3.2, and 3.4, while cluster 3.3 is more repulsive in 5–8 planes at the on-mirror positions. Clusters 3.1 and 3.4 are more repulsive in the fifth plane at the off-mirror sites, and almost all tri-vacancy clusters are less repulsive in the seventh and the eighth planes.

Effects of temperature on the interaction energy for single-, di-, and tri-vacancies are calculated near the (1 2 0) twin boundary in the first pane at the temperature ranging from 0 K to 1000 K in steps of 100 K (see Figs. 2–4). Clusters 1.1, 2.1, and 3.1 have the interaction energies of −0.07367 eV,

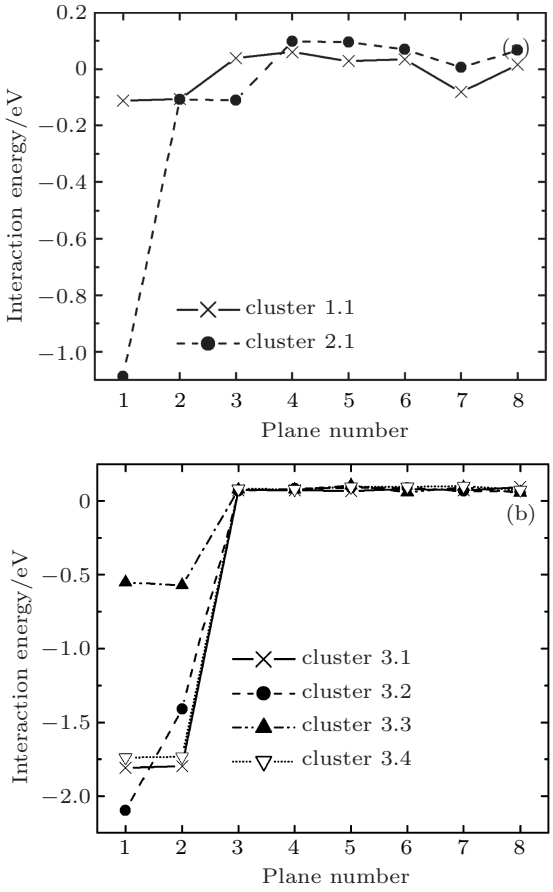

Fig. 8. Interaction energies of (a) single- and di-vacancies and (b) four tri-vacancy clusters in different planes near the (1 2 0) twin boundary at 300 K.

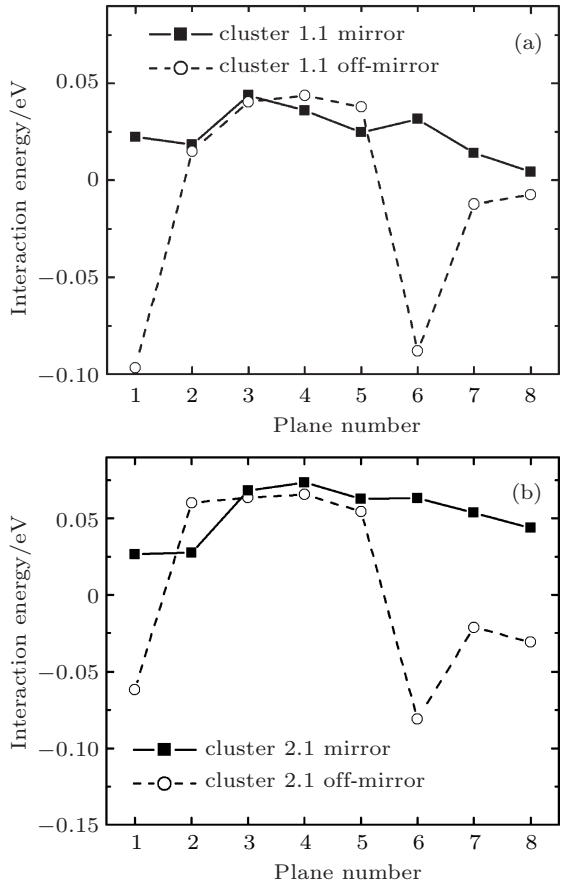

Fig. 9. Interaction energies of (a) single-vacancy and (b) di-vacancy clusters on either side of the (1 2 0) twin boundary at 300 K.

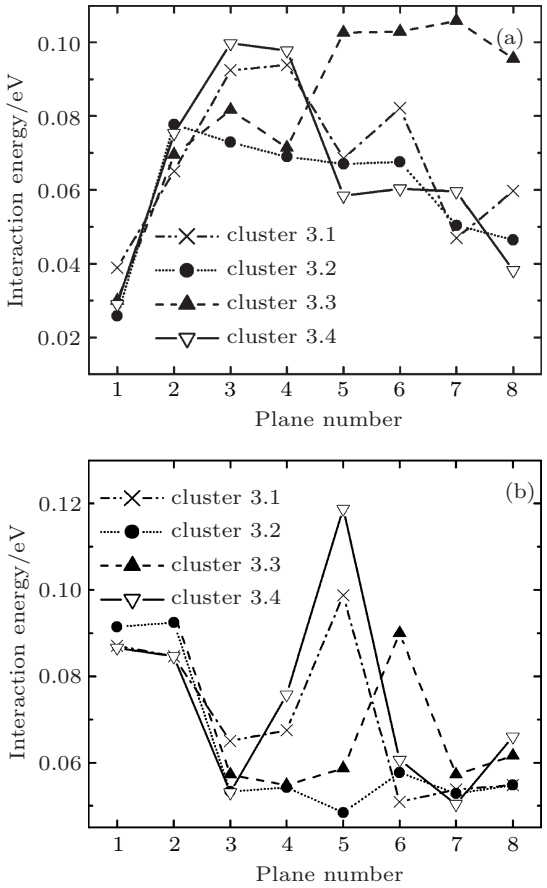

Fig. 10. Interaction energies of tri-vacancy clusters at 300 K on either side of (1 2 0) twin boundary at (a) on- and (b) off-mirror sites.

−1.21345 eV, and −1.94543 eV, respectively, at 0 K. In the closest plane near the (1 2 0) twin boundary, all these vacancy clusters present attractive behaviors. However, with the increase in temperature, the interaction energy increases and attraction reduces. The interaction energies averagely change by 0.006697 eV, 0.110314 eV, and 0.176857 eV for clusters 1.1, 2.1, and 3.1, respectively, with a 100 K increase in temperature. The interaction energies become −0.04176 eV, −0.14568 eV, and −1.03448 eV for single-, di-, and tri-vacancies, respectively, at 1000 K.

The interfaces with high atomic density each have a large interplanar spacing and vice-versa. The atomic relaxation of a plane is proportional to the interplanar spacing and inversely proportional to the atomic density in that plane. Therefore, the interfaces with low atomic density have high twin formation energy and vice-versa. The disturbance of atoms is maximum at the interface, while the other part of the crystal is perfect. Therefore, the plane registry and interlayer relaxations decrease with movement away from the interfaces and after a dozen of planes become negligible. The interplanar spacing and energy per atom increase with the increase in temperature. With large distances between atoms and high energy, the generation of twins and the relaxation in the crystal both become easy. Therefore, the twin formation energy decreases with the increase in temperature.

Considerable relaxations can be seen near the (1 1 3) and (1 2 0) twin boundaries. Compact interfaces relax less than the high-index interfaces because of the lack of symmetry in high-index interfaces.[18,38] The (1 2 0) interface is more open (has a lower atomic density) than the (1 1 1) and (1 1 3) interfaces. Therefore, comparatively strong relaxation is found near the (1 2 0) twin boundary. The interplanar spacing of the (1 1 3) interface is less (0.2761α) than that of the (1 1 1) interface and the relaxation is easy near the (1 1 3) twin boundary compared with the (1 1 1) interface. Therefore, the (1 1 1) interface shows a repulsive behavior and the (1 1 3) interface presents an attractive behavior for vacancy clusters. The bulk atoms have electric and ionic symmetry arrangements throughout the bulk; therefore, some modifications are required in the charge configuration near the interface. The force field changes compared with the bulk atoms with normal coordinates. Some relaxations appear as the field changes; the interlayer spacing changes around these twin interfaces. During the planes moving in the direction perpendicular to the interface, the registry of atomic planes may be changed due to the relaxation of planes in the direction parallel to the boundary. A proper charge redistribution around the grain boundaries is facilitated by these multilayer relaxations. In the process of relaxation, the spacing around the twin interface relaxes more than the bulk interplanar spacing. Since at the interfaces, the atomic density is less (coordinates less than 12 which is required for

the fcc crystal) than that in the bulk (normal coordinates), the relaxation is easy near the interface. Therefore, most vacancy clusters feel more attractive in the planes closest to the interface and less attractive or repulsive with away from it. It means that the vacancy clusters tend to move towards the twin interfaces. Although the relaxation is easy at high temperature, with the increase in temperature, energies and dynamic behaviors (repulsion) of atoms increase. Therefore, almost for all vacancy clusters, the interaction energy increases at high temperatures.

The convergences of interaction energies with respect to the system size for all twin boundaries are checked. Enough planes are taken along the fixed boundary and the use of periodic boundary conditions along two dimensions diminishes the effect of size of the crystal on calculations. The results presented in this work are reliable as they have been obtained using a well established set of computer programs, which have produced reasonable results for other fcc metals.[11,16–19,36,37,39–43] The simulated results of interaction energy with twin boundaries of vacancy clusters are satisfactory in the sense that the atomic relaxations are all consistent with what might be anticipated using the hard sphere model and are comparable to the results of the previous findings.[32,36]

4. Conclusions

We conclude that the twin formation energy decreases with the increase in temperature for the (1 1 3) and (1 2 0) twin boundaries, except for the (1 1 1) twin boundary. This decreasing trend is more prominent for the (1 2 0) twin boundary than that for the (1 1 3) twin boundary. The (1 1 1) twin interface has a low twin formation energy, and there is no considerable interlayer and registry relaxations around the twin interface due to the comparatively high planar atomic density and larger interplanar. The (1 2 0) twin interface has a high twin formation energy and shows greater interlayer and registry relaxations around the twin interface. Almost all vacancy clusters are favorable in the closest planes and the repulsion increases as they move away from the boundaries at on- and off-mirror sites, except tri-vacancies near the (1 2 0) interface at off-mirror sites and clusters 3.3 and 3.4 at on- and off-mirror sites near the (1 1 1) interface. The on-mirror arrangements are favorable for all vacancy clusters near the (1 1 3) twin boundary. Single- and di-vacancies are more favorable at the on-mirror sites near the (1 1 1) twin boundary, while these are attractive at the off mirror sites near the (1 2 0) twin boundary. At high temperatures, the attraction decreases for all vacancy clusters, except for the single vacancy near the (1 1 1) interface.

References

[1] Chris D G, Parfenov A, Gryczynski I and Lakowicz J R 2003 *Chem. Phys. Lett.* **380** 269
[2] Hutchings G J 2009 *Gold Bull.* **42** 260
[3] Kartusch C and van Bokhoven J A 2009 *Gold Bull.* **42** 343
[4] Bond G and Thompson D 2009 *Gold Bull.* **42** 247
[5] Zijlstra P, Chon J W M and Gu M 2009 *Nature* **459** 410
[6] de las Heras N, Roberts E P L, Langton R and Hodgson D R 2009 *Energy & Environmental Science* **2** 206
[7] Kumar A, Ricketts M and Hirano S 2010 *Journal of Power Sources* **195** 401
[8] Link S, Burda C, Nikoobakht B and El-Sayed M A 1999 *Chem. Phys. Lett.* **315** 12
[9] Crocker A G 1975 *Philos. Mag.* **32** 379
[10] Crocker A G and Faridi B A 1980 *Acta Metall.* **28** 549
[11] Noorullah, Akhter J I and Yaldram K 1997 *The Nucleus* **34** 17
[12] Van Swygenhoven H and Derlet P M 2001 *Phys. Rev. B* **64** 224105
[13] Daw M S and Baskes M I 1984 *Phys. Rev. B* **29** 6443
[14] Park H S, Gall K and Zimmerman J A 2006 *Mech. Phys. Solids* **54** 1862
[15] Lutsko J F, Wolf D, Phillpot S R and Yip S 1989 *Phys. Rev. B* **40** 2841
[16] Akhter J I, Ahmed E and Ahmad M 2005 *Mater. Chem. Phys.* **93** 504
[17] Ahmed E, Akhter J I and Ahmad M 2004 *Comput. Mater. Sci.* **31** 309
[18] Hayat S S, Choudhry M A, Hussain A, Alam S, Ahmad S A and Ahmad I 2009 *Ind. J. Pure Appl. Phys.* **47** 730
[19] Hayat S S, Choudhry M A and Ahmad S A 2008 *J. Mater. Sci.* **43** 4915
[20] Weidersich H 1992 *Mat. Sci. Division* 6043
[21] Suzuki A and Mishin Y 2003 *Inter. Sci.* **11** 425
[22] Bacon D J and Osetsky Yu N 2005 *Mat. Sci. Engg.* **400** 353
[23] Serra A and Bacon D J 2008 *Multiscale Material Modeling* p. 803
[24] Van Swygenhoven H and Weertman J R 2003 *Scripta Mater.* **49** 625
[25] Schiøtz J and Jacobsen K W 2003 *Science* **301** 1357
[26] Wang J, Tian M, Mallouk T E and Mose H W 2004 *Can. J. Phys. Chem. B* **108** 841
[27] Toimil Molares M E, Van Buschmann D D, Neumann R, Scholz R, Schuchert I U and Vetter J 2001 *Adv. Mater.* **13** 62
[28] Sauer G, Brehm G, Schneider S, Nielsch K, Wehrspohn R B, Choi J, Hofmeister H and Gösele U J 2002 *Appl. Phys.* **91** 3243
[29] Ahmed S A, Crocker A G and Faridi B A 1983 *Philos. Mag. A* **48** 31
[30] Crocker A G and Faridi B A 1978 *J. Nucl. Mater.* **69/70** 671
[31] Crocker A G and Faridi B A 1980 *Acta Metall.* **28** 549
[32] Ahmad S A and Ramzan R 2007 *Chin. Phys. Lett.* **24** 2631
[33] Murr L E 1972 *Scripta Metall.* **6** 203
[34] Nordsieck A 1962 *Math. Comput.* **16** 22
[35] Fletcher R 1972 *A FORTRAN subroutine for minimization by the method of conjugate gradients* AERE–R7073
[36] Hussain F, Hayat S S and Imran M 2011 *Physica B* **405** 1060
[37] Hayat S S 2011 *Computational Materials Science* **50** 1485
[38] Yıldırım H and Durukanoğlu S 2003 *ARI, Bull Istanbul Tech. Univ.* **53** 53
[39] Akhter J I, Yaldram K and Ahmad W 1996 *Sol. Stat. Comm.* **98** 1043
[40] Hayat S S, Choudary M A, Ahmad S A, Akhter J I and Hussain A 2008 *Ind. J. Pure Appl. Phys.* **46** 771
[41] Akhter J I and Yaldram K 1997 *Int. J. Mod. Phys. C* **8** 1217
[42] Hayat S S, Alcántara Ortigoza M, Choudary M A and Rahman T S 2010 *Phys. Rev. B* **82** 085405
[43] Faridi B A S, Ahmad S A and Choudhry M A 1991 *Ind. J. Pure Appl. Phys.* **29** 796